

Introduction

- Fe-Al and Ni-Al mixed oxide nanoparticles were synthesized over a range of compositions (0-100% Al) via a resin-gel method.
- It was expected that Fe/Al and Ni/Al would form a defect spinel structure in solid solution, as observed in the bulk.
- Characterisation was carried out by powder X-ray diffraction (PXRD), transmission electron microscopy (TEM), and energy dispersive X-ray spectroscopy (EDS).

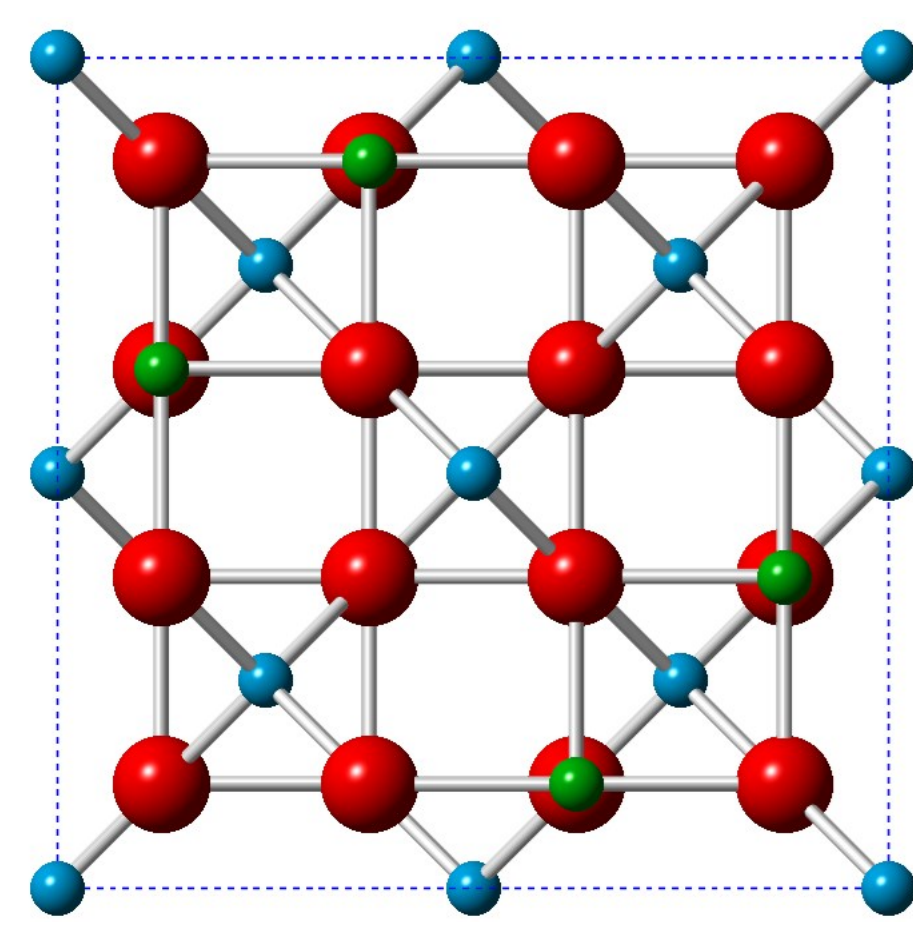


Figure 1. The spinel structure¹, viewed down <100>. Anions in red, tetrahedral sites in blue, octahedral sites in green.

Resin-Gel Method²

1. Metal salts of Fe-Al and Ni-Al were dissolved in solution.

2. Polyethylene glycol (PEG, MW = 20,000) was added to solution in a 1:1 volume ratio.

4. Samples were calcined under flowing O₂ (Fe-Al 500 °C; Ni-Al 400 °C) for 1 week.

3. The resin was dried in ambient conditions to form a waxy solid, then pyrolyzed.

Ni-Al Oxide Nanoparticles

PXRD:

- PXRD identified only peaks corresponding to the bunsenite rocksalt structure. No additional peaks due to the spinel structure were observed.
- For the Al-rich end only an amorphous signal was observed.

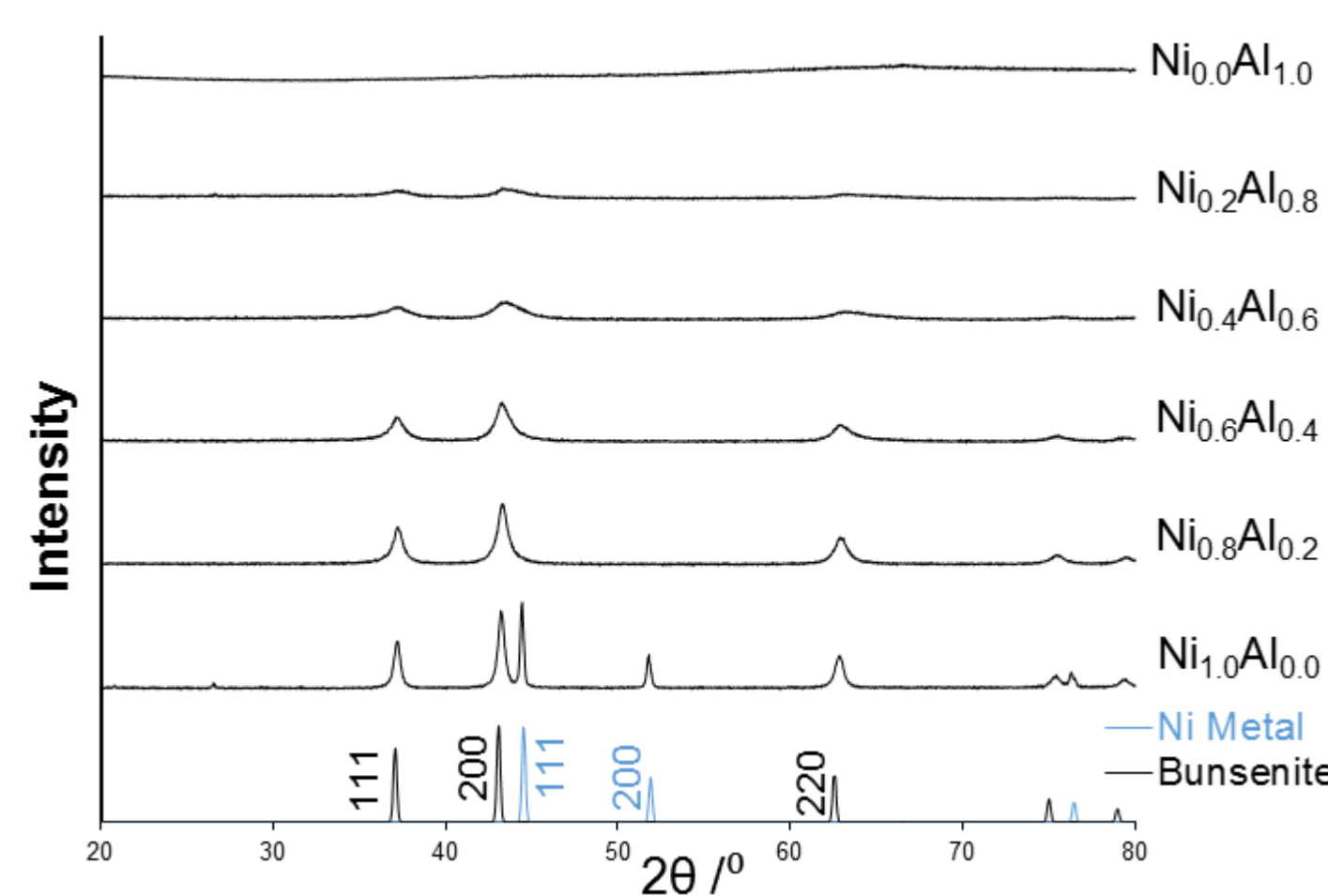


Figure 2. PXRD spectra for all six compositions of Ni-Al mixed oxides, with bunsenite³ (NiO, rocksalt structure) and Ni metal⁴ references along the x-axis.

EDS and TEM:

- EDS confirmed the synthesis of mixed metal oxides.
- Spherical structures of amorphous material were observed in the TEM, for Al-rich samples, that contained no distinguishable internal structure.
- Lattice planes identified in the images could be indexed to the bunsenite structure, with no additional peaks due to the spinel structure being observed, suggesting the relative stability of the bunsenite structure at low temperature.
- Crystals of pure NiO were identified in all Ni containing samples across the compositional range.

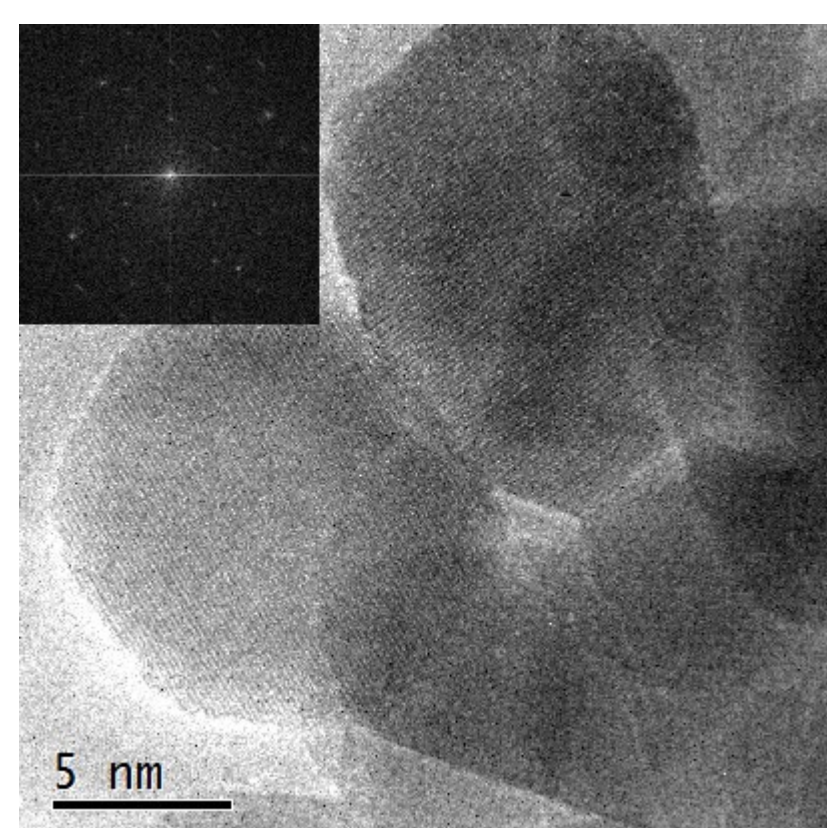


Figure 3. Micrograph of hexagonal NiO nanocrystals (5-30 nm) from the pure NiO sample. $d_{220} = 1.54 \text{ \AA}$.

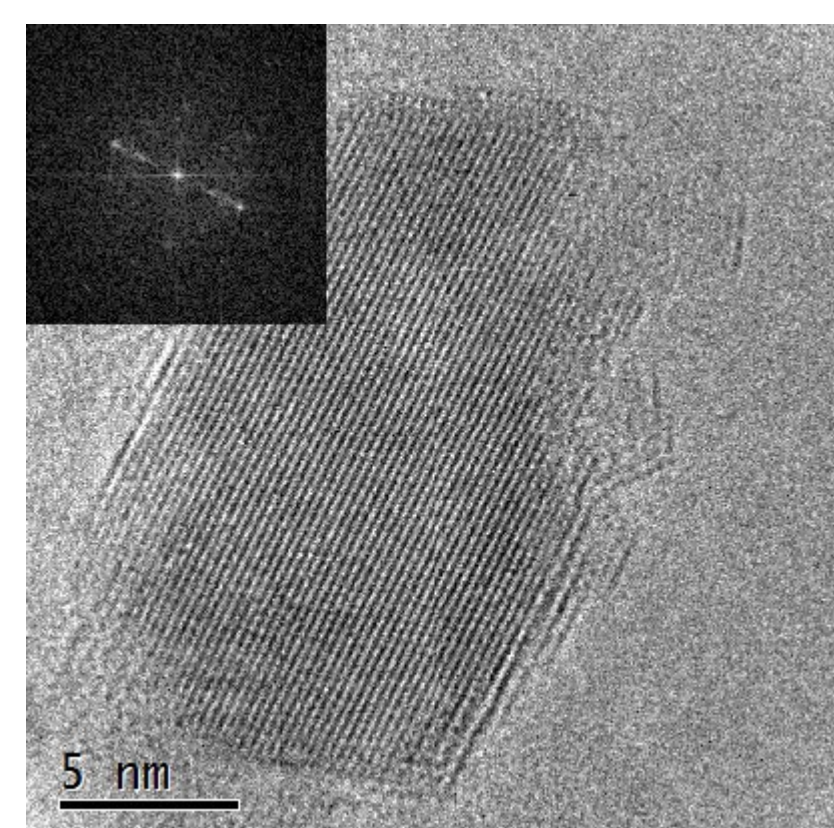


Figure 4. Micrograph of a nanocrystal of the bunsenite phase in Ni_{0.6}Al_{0.4}, with no clear crystal morphology. $d_{111} = 2.46 \text{ \AA}$; $d_{200} = 2.19 \text{ \AA}$; $d_{111} = 2.50 \text{ \AA}$.

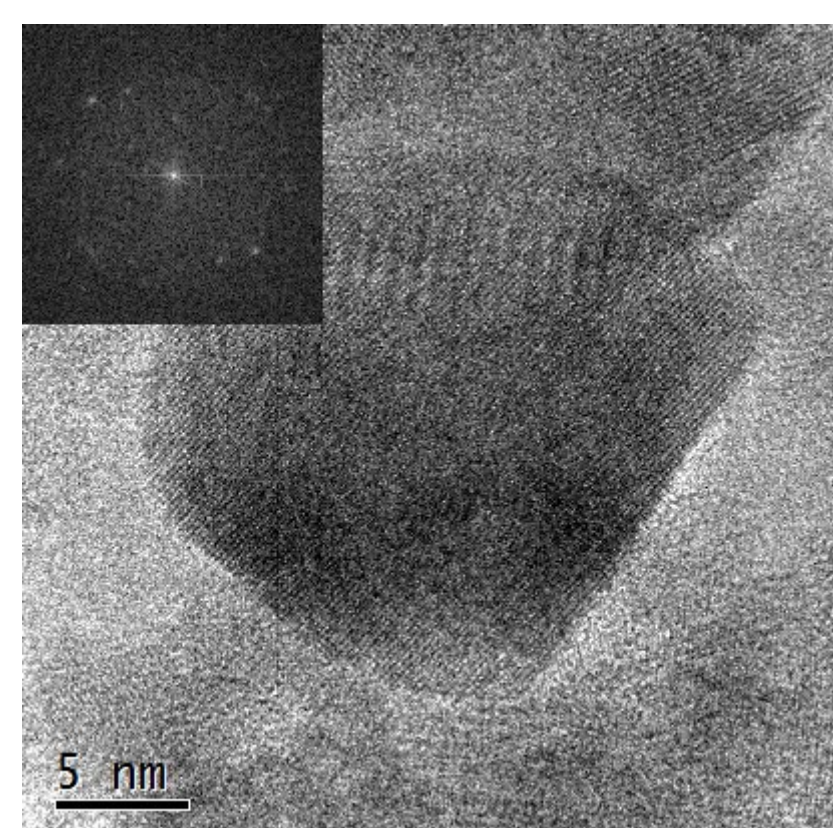


Figure 5. Micrograph of nanocrystals of the main phase in Ni_{0.4}Al_{0.6}, with no clear morphology. $d_{111} = 2.46 \text{ \AA}$; $d_{200} = 2.19 \text{ \AA}$; $d_{220} = 1.54 \text{ \AA}$.

Discussion

- For the Ni-Al system, no lattice planes indicative of the spinel structure were observed. In the low temperature limit, the bunsenite structure forms preferentially owing to the tendency of Ni^{II} to occupy octahedral rather than tetrahedral sites.
- For the Fe-Al system, the spinel structure was observed for mixed oxide nanoparticles, but at high Fe content, another phase with the hematite structure also formed. Amorphous material was formed for all mixed systems.

Fe-Al Oxide Nanoparticles

PXRD:

- Samples with under 40% Fe were identified as amorphous.
- Samples with over 40% Fe contained peaks corresponding to the spinel structure.
- Samples with over 80% Fe showed the presence of another phase with the hematite structure.
- Scherrer analysis estimated a particle size of 3-5 nm.

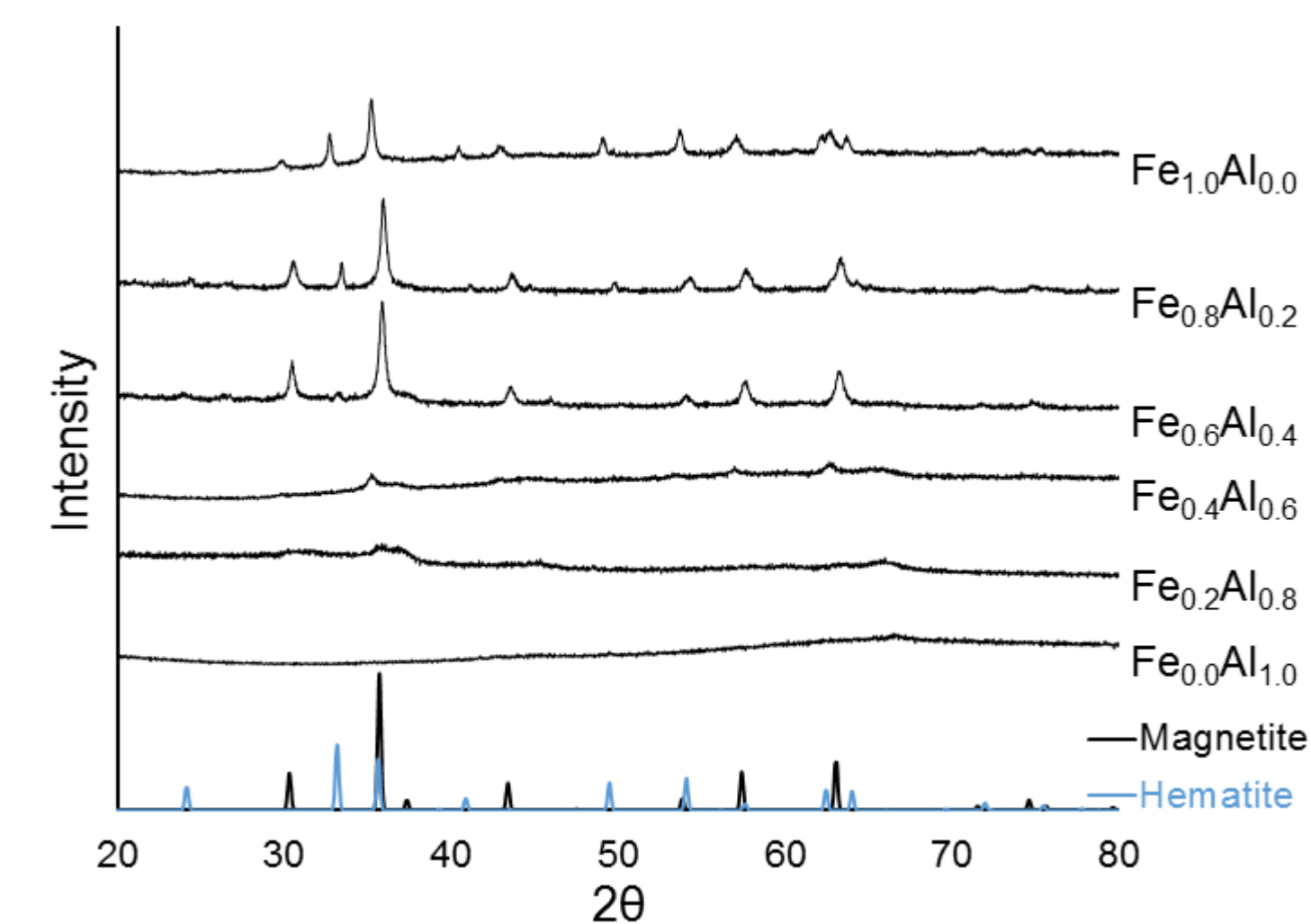


Figure 6. PXRD spectra for all six compositions of Fe-Al mixed oxides, with magnetite (Fe₃O₄, spinel structure¹) and hematite (Fe₂O₃, corundum structure⁵)

EDS and TEM:

- EDS confirmed the synthesis of mixed metal oxide nanoparticles.
- TEM micrographs suggested a particle size of 5-20 nm.
- Micrographs suggested that all of the samples contained amorphous material, but became more crystalline as the Fe content increased. The amorphous phase composition could not be determined due to the impossibility of single crystal EDS analysis.
- The phases found via EDS/TEM agreed with observations from PXRD, and are summarized in Figure 7.

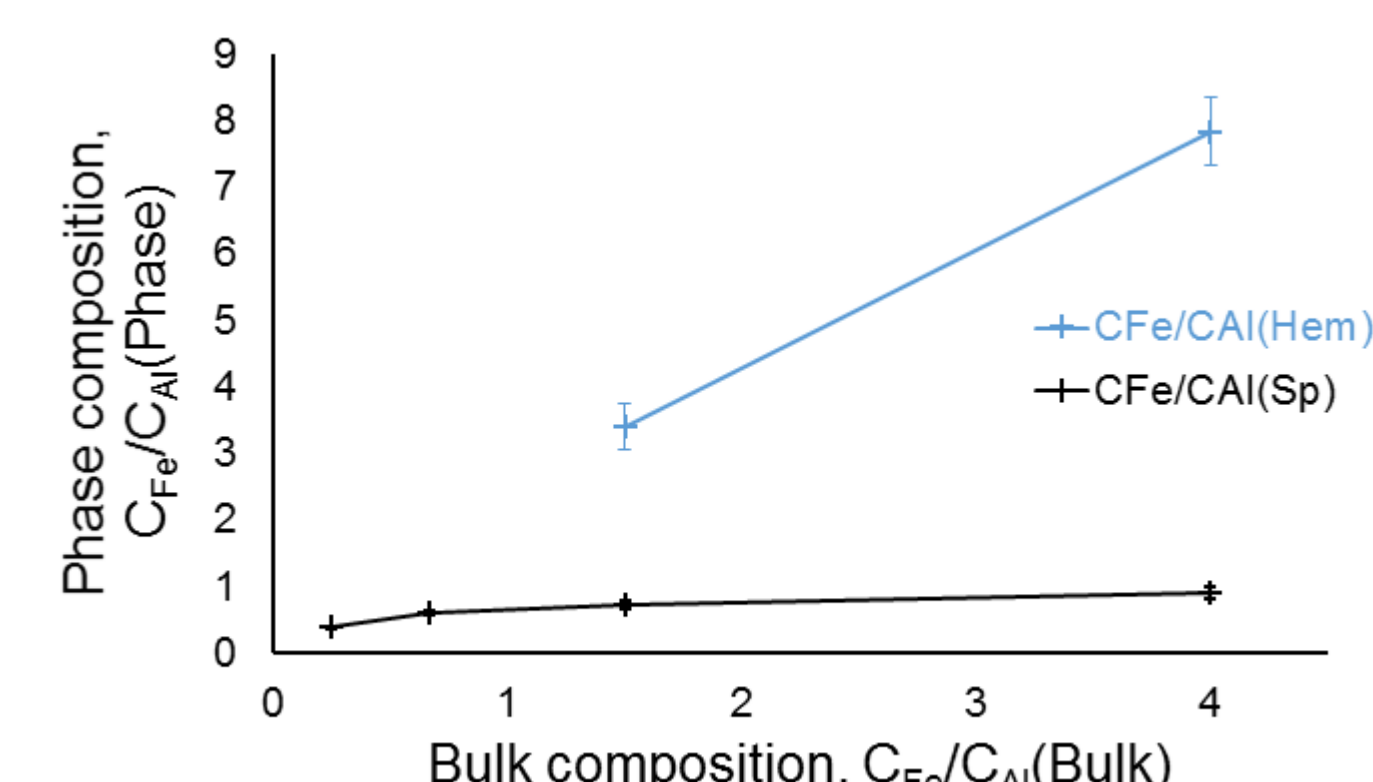


Figure 7. Summary of the composition of the crystalline phases found across all bulk compositions. Hematite in blue, spinel in black.

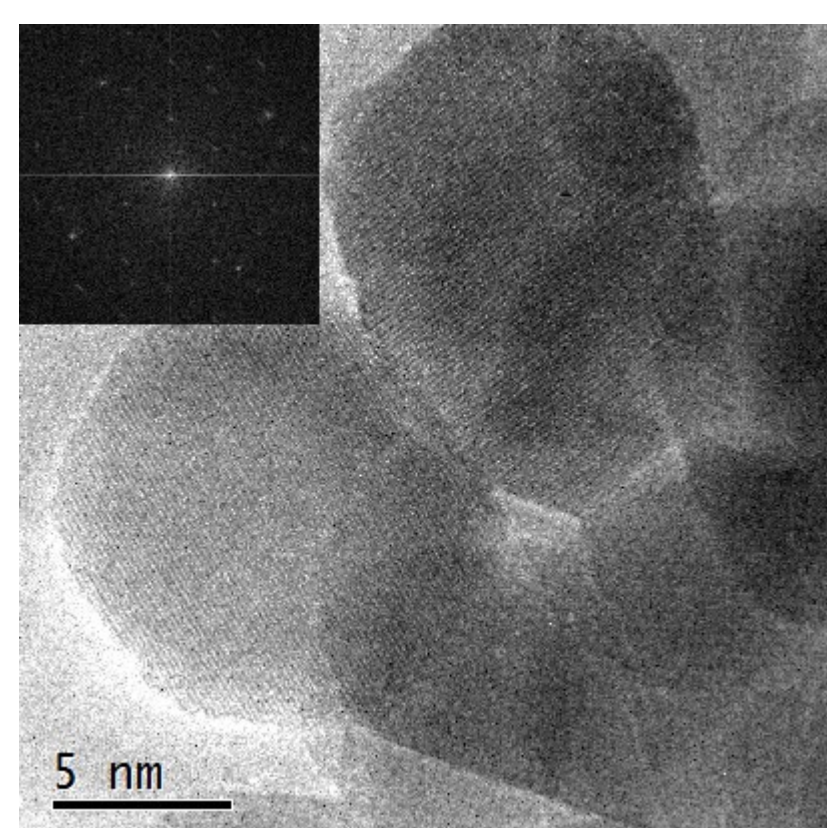


Figure 8. Micrograph of Fe_{0.2}Al_{0.8}. The sample is mainly amorphous.

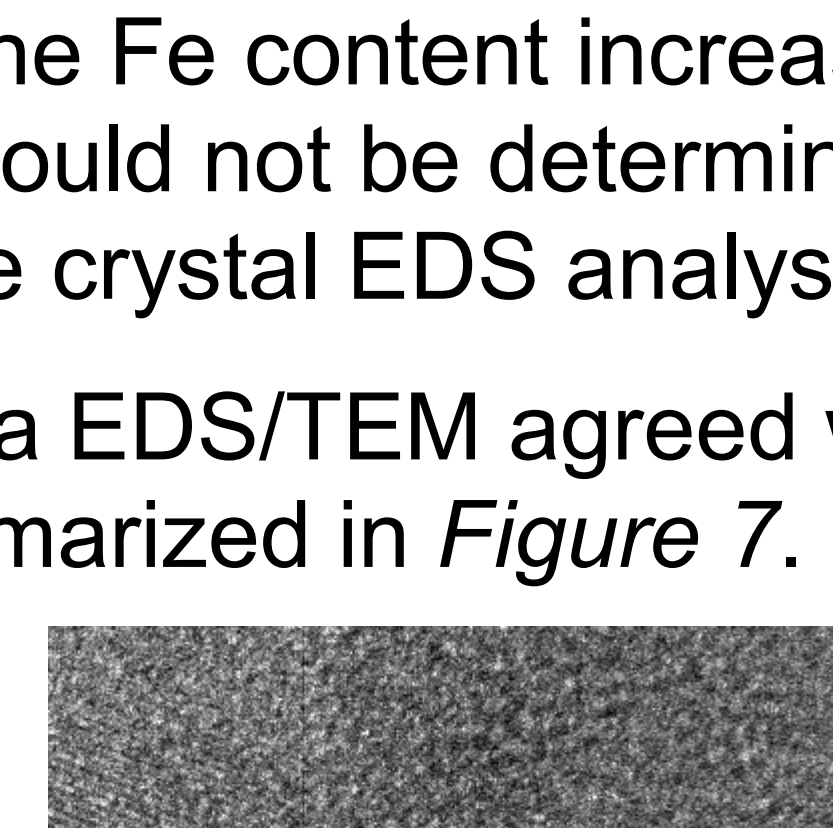


Figure 9. Micrograph of Fe_{0.6}Al_{0.4}. Nanocrystals are embedded in an amorphous matrix: $d = 2.13 \text{ \AA}$ (d_{400} spinel) $d = 2.60 \text{ \AA}$ (d_{311} spinel or d_{110} hematite).

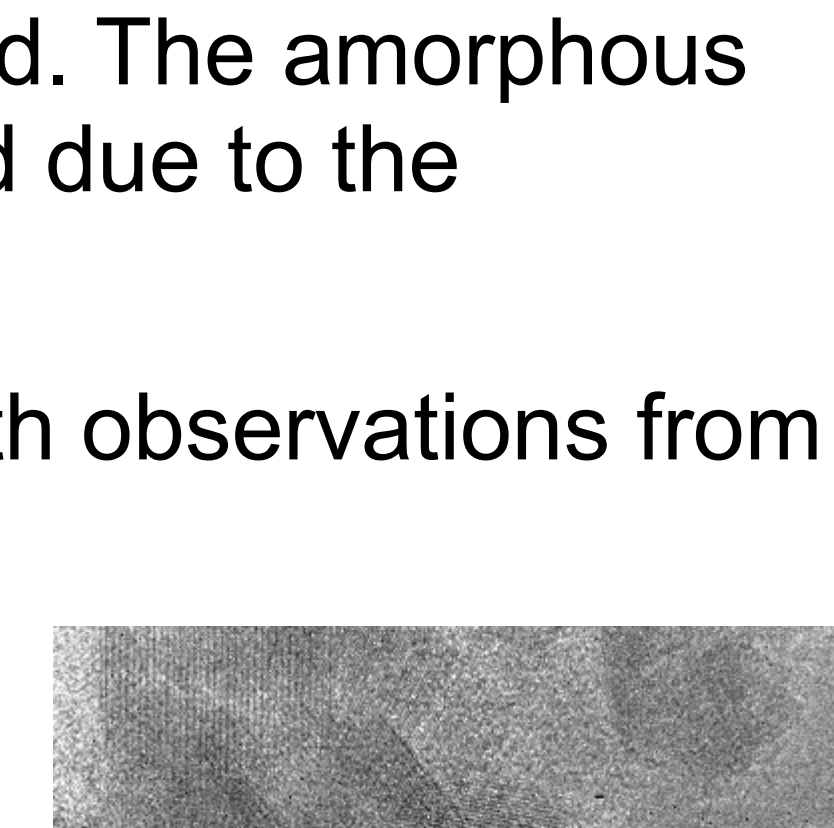


Figure 10. Micrograph of Fe_{1.0}Al_{0.0}. The pure iron sample is fully crystalline.

References

- (1) W.H. Bragg, *Nature*, 95, 561, (1915); (2) X. Li, H. Zang, F. Chi, S. Li, B. Xu and M. Zhao, *Mat. Sci. Eng. B.*, 10, 209-213, (1993); (3) W.P. Davey, E.O. Hoffmann, *Phys. Rev.*, 15, 333, (1920); (4) E.R. Jette, F. Foote, *J. Chem. Phys.*, 3, 605-616, (1935); (5) L. Pauling, *J. Am. Chem. Soc.*, 47, 781-790, (1925).